

## INTERGRANULE FUSION IN RAT *PARS INTERMEDIA* CELLS

KATARINA KOŠMELJ<sup>1</sup>, ANTON CEDILNIK<sup>1</sup>, PETER VERANIČ<sup>2</sup>, GREGOR ZUPANČIČ<sup>3</sup>, MARJAN RUPNIK<sup>3</sup>, LAURA KOČMUR-BOBANOVIČ<sup>3</sup> AND ROBERT ZOREC<sup>3</sup>

<sup>1</sup>Biotechnical Faculty, University of Ljubljana, Jamnikarjeva 101, 1111 Ljubljana, Slovenia, <sup>2</sup>Institute of Cell Biology, Medical School, Lipičeva 5, 1001 Ljubljana, Slovenia, <sup>3</sup>Laboratory of Neuroendocrinology-Molecular Cell Physiology, Institute of Pathophysiology, Medical School, P.O. Box 2211, 1001 Ljubljana, Slovenia  
e-mail: robert.zorec@pafi.mf.uni-lj.si  
(Accepted April 26, 2001)

### ABSTRACT

Using electron microscopy, we studied the morphology of secretory granules in rat *pars intermedia* cells. We found figures of apparent intergranule fusion, characterized by a tight association of two granules. The fusion was detected in around 2% of all measured granules, indicating a low occurrence of intergranule fusion. To study whether intergranule fusion affects the distribution of granule diameters a simple probabilistic model was developed. It is based on the theory that larger granules are formed by fusion of two or more spherical granules of fixed size, and that the surface of a newly formed granule is equal to the sum of fused granule membranes. The model accounts for the bias on granule diameter measurements due to sectioning of granules. Although the electron microscopy data strongly indicates the existence of intergranule fusion in rat melanotrophs, this process as modelled in the present work does not contribute to the granule diameter distribution significantly. It is likely that in addition to the fusion of larger granules, other processes, such as fusion of microvesicles, may affect the distribution of granule diameters.

Keywords: intergranule fusion, melanotrophs, probabilistic model, rat, secretory granules, stereology.

### INTRODUCTION

Cells from the rat *pars intermedia* secrete a number of peptides deriving from post-translational processing of pro-opiomelanocortin (POMC), including  $\beta$ -endorphin,  $\alpha$ -melanocyte stimulating hormone ( $\alpha$ -MSH) and adrenocorticotrophin (ACTH, Mains and Eipper, 1979). The formation of peptide-containing secretory granules begins with the condensation of secretory products within the lumen of the trans-Golgi network, followed by budding of immature secretory granules (Tooze, 1991). During the maturation process the size of secretory granules is increasing (Farquhar *et al.*, 1978; Tooze *et al.*, 1991), and in rat melanotrophs their cargo is undergoing metabolic changes (Tanaka *et al.*, 1991). Larger granules possibly result from fusion between smaller granules of unitary size (Alvarez de Toledo and Fernandez, 1990; Hartmann *et al.*, 1995). The size of larger granules may also be influenced by the fusion of microvesicles with secretory granules. Microvesicles are thought to be trafficking between secretory granules and other compartments (Tooze and Tooze, 1986; Komuro *et al.*, 1987).

The size of the secretory granules in rat *pars intermedia* depends on physiological state of the animal. It is reduced when the animal is pretreated with bromocriptine (Bäck, 1989). However, an increase of granules was reported in hypersecretory melanotrophs. It could be due to mechanisms operating at an early stage of granule formation (Bäck and Sojnila, 1994).

In the present study we use electron microscopy to examine the morphology of secretory granules in rat *pars intermedia* cells. We detected some apparent intergranule fusions. The main objective of our study was to find out if granule growth is associated with fusion of unitary granules (Alvarez de Toledo and Fernandez, 1990; Hartmann *et al.*, 1995). If this is the dominant process in granule diameter growth in rat melanotrophs, robust peaks in the multimodal distribution of granule diameters are anticipated.

The reported distributions of granule profile diameters in rat melanotrophs are heterogeneous (Bäck, 1989; Zupančič *et al.*, 1994). The previous electrophysiological experiments (Zupančič *et al.*, 1994) were not sufficiently sensitive, therefore we

studied secretory granule morphology by electron microscopy. To analyse the granule diameter distribution we developed a simple probabilistic model assuming that larger granules are formed by fusion of two or more spherical granules of fixed size, and that the surface of a newly formed granule is equal to the sum of fused granule membranes. The model also accounts for the bias due to the sectioning of embedded specimens prepared for electron microscopy, a standard stereological problem.

## MATERIAL AND METHODS

### CELL PREPARATION, ELECTRON MICROSCOPY AND MEASUREMENTS OF GRANULE DIAMETERS

After ether anaesthesia animals (male Wistar rats, 200 to 300 g) were killed by decapitation. *Pars intermedia* of each animal was carefully dissected from the pituitary gland and divided into 4 to 6 pieces of tissue in Earl's Balanced Salt Solution (EBBS, Sigma Chemical Co., USA). Tissue pieces were maintained in a culture medium (Rupnik and Zorec, 1992), placed in an incubator (36°C, 4.6% CO<sub>2</sub>) for 24 hours, and then fixed in buffered (pH 7.3) 0.5% glutaraldehyde with 0.5% tannic acid for 30 minutes at room temperature. After that the tissue was fixed for an hour in buffered (pH 7.3) 2.5% glutaraldehyde without tannic acid. After the postfixation in 2% osmium tetroxide with 3% ferrocyanide tissue pieces were immersed in 1% water solution of uranyl acetate for 30 minutes in darkness. After dehydration the tissue was embedded in Epon 812 (Medium grade, London Resin Co, U.K.). Ultrathin sections (70 nm) were cut with a LKB ultramicrotome and examined with a Jeol T8 transmission electron microscope.

Diameters of secretory granule profiles were measured in mm from electron micrographs, enlarged to the scale of 126 000. The smallest detectable profile diameter was 8 mm (64 nm). The accuracy of the data readings was  $\pm 1$  mm (8 nm). Some of the profiles appeared non-spherical, their maximal diameter was measured.

## THEORETICAL MODEL

### Sectioning Process

Let us assume a population of sphere granules all having an equal diameter  $D$ . Granules are cut by parallel random planes (Fig. 1A). For each granule, parallel cuts are uniformly distributed on the granule diameter. Diameters of the obtained sphere profiles ( $d$ ) are measured.

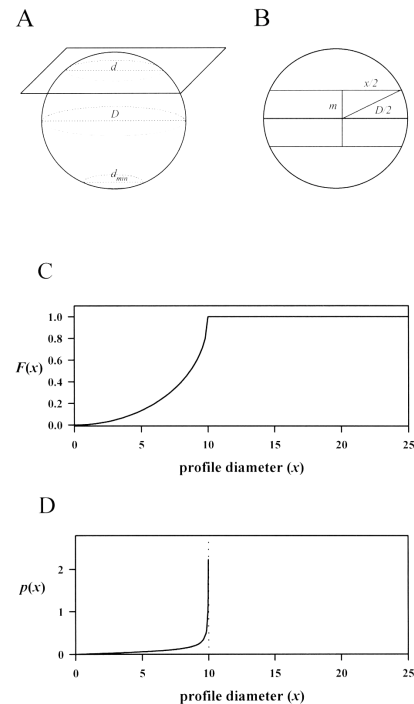


Fig. 1. **A** presents a diagram of sectioning a spherical secretory granule with diameter  $D$ . On each sphere profile its diameter  $d$  is measured. The smallest detectable profile diameter is  $d_{min}$ . **B** The distribution function  $F(x)$  is obtained on the basis of this plot, from the right-angled triangle with sides  $D/2$ ,  $m$  and  $x/2$  (see Material and Methods, Theoretical Models, Sectioning Process). **C** A distribution function  $F(x)$  for profile diameters is  $D = 10$  (arbitrary units). The smallest detectable profile diameter is  $d_{min} = 0$ . **D** Probability density function  $p(x)$  for profile diameters. The granule diameter is  $D = 10$  (arbitrary units). The smallest detectable profile diameter is  $d_{min} = 0$ .

Profile diameter  $d$  can be regarded as a random variable with values ranging from 0 to  $D$ . Its distribution function<sup>1</sup>,  $F(x)$ ,  $0 < x < D$  is obtained geometrically from a right-angled triangle with sides  $D/2$ ,  $m$  and  $x/2$  (Fig. 1B). It is:

$$F(x) = 1 - \frac{2m}{D} = 1 - \frac{\sqrt{D^2 - x^2}}{D}.$$

Profile diameters smaller than a particular value can not be detected reliably in experimental work. Let us denote the smallest detectable diameter  $d_{\min}$ ; its value is known from the experimental technique. Then the distribution function is:

$$F(x) = 1 - \sqrt{\frac{D^2 - x^2}{D^2 - d_{\min}^2}}, \quad d_{\min} < x < D. \quad (1)$$

Differentiation of Eq. 1 gives the probability density function<sup>2</sup>  $p(x)$ :

$$p(x) = \frac{x}{\sqrt{(D^2 - d_{\min}^2)(D^2 - x^2)}}, \quad d_{\min} < x < D \quad (2)$$

A pole at  $x = D$  should be noted. For illustration we present  $F(x)$  and  $p(x)$  on Fig. 2. It turns out that the expected value of  $d$  is:

$$E(d) = \int_{d_{\min}}^D xp(x)dx = \frac{d_{\min}}{2} + \frac{D^2}{2\sqrt{D^2 - d_{\min}^2}} \arccos \frac{d_{\min}}{D}. \quad (3)$$

Since  $E(d)$  is an increasing function of  $d_{\min}$ , its infimum is:

$$\inf E(d) > \frac{\pi}{4} D.$$

Thus, the average value of profile diameters is approximately  $\pi/4$  of  $D$  for small  $d_{\min}$ , consistent with Weibel (1979). These results provide theoretical background for the graphical methods commonly used in stereology.

### Fusion Effect Model

This model describes the fusion theory as follows. The smallest granules, i.e., unit granules, fuse into double, triple, ... granules. The maximal granule size type  $K$  is unknown. For simplicity reasons we assume that the unit granules are spherical, their diameter  $D_1$  fixed but unknown. Following the intergranule fusion theory, the surface of the granule size type  $k$ , say  $S_k$ ,

is,  $S_k = kS_1$ ,  $k = 1, \dots, K$  and consequently its diameter  $D_k = \sqrt{k}D_1$ .

Fusion is a rare event. Therefore, we assume that the probability of fusion into a granule type  $k$ ,  $p_k$ , follows a finite Poisson-like distribution:

$$p_k = \alpha_K \frac{\lambda^{k-1}}{(k-1)!}, \quad k = 1, 2, \dots, K, \quad (4a)$$

Probability  $p_k$  describes the fraction of type  $k$  granules. It can be shown that  $\lambda$  is the unknown parameter representing the expected granular size type in the following way:

$$E_K(k) \approx 1 + \lambda,$$

and  $\alpha_K$  is the normalizing constant:

$$\alpha_K = \left( 1 + \frac{\lambda}{1} + \frac{\lambda^2}{2} + \dots + \frac{\lambda^{K-1}}{(K-1)!} \right)^{-1}.$$

These granules undergo the sectioning process described previously. i.e. granules are cut by parallel random planes. For each granule, parallel cuts are uniformly distributed on the granule diameter. Diameters of the obtained sphere profiles are measured. We denote by  $q_k$  the probability that a granule of type  $k$  is hit by a random plane. This probability is proportional to the granule's diameter:

$$q_k \propto \sqrt{k}D_1$$

and to the proportion of granules of type  $k$ :

$$q_k \propto p_k$$

It turns out, that  $q_k$  is as follows:

$$q_k = \frac{p_k \sqrt{k}}{\sum_{k=1}^K p_k \sqrt{k}}, \quad k = 1, \dots, K \quad (4b)$$

Following Eq. 1, the distribution function for any granular size type  $k$  is:

$$F_k(x) = 1 - \sqrt{\frac{kD_1^2 - x^2}{kD_1^2 - d_{\min}^2}}, \quad d_{\min} < x < \sqrt{k}D_1. \quad (5)$$

Pooling together all the granular size types with the corresponding probabilities  $q_k$  (Eq. 4b) gives the global distribution function  $G(x)$ :

<sup>1</sup> Distribution function  $F(x)$  gives the probability that a random variable  $X$  takes a value less than  $x$ ,  $F(x) = P(X < x)$ .

<sup>2</sup> Probability density function  $p(x)$  is obtained as the derivative of  $F(x)$ .

$$G(x) = \sum_{k=1}^K q_k F_k(x). \quad (6)$$

$G(x)$  is of saw-tooth shape. Fig. 2 illustrates  $G(x)$  graphically. Relative cumulative function estimates the distribution function  $G(x)$ , which is nonlinear.

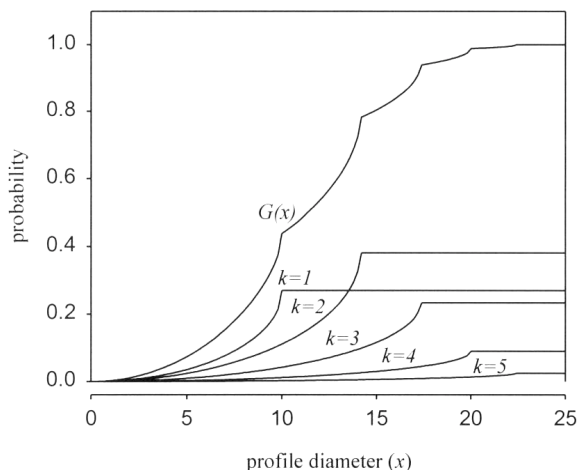


Fig. 2. Presents distribution function  $G$  and its components based on Model 1. The following values of parameters are taken into account:  $D_1 = 10$  (arbitrary units),  $\lambda = 1$ ,  $K = 5$ . The smallest detectable profile diameter is  $d_{min} = 0$ .

The parameters to be estimated are  $D_1$  and  $\lambda$ . Their starting values can be estimated from the empirical distribution of profile diameters: starting value for  $D_1$  corresponds to the abscissa of the first observable peak,  $\lambda$  to the granular size type with the highest frequency. A number of numerical techniques may be applied to find the least squares estimates commonly used in regression models (Everitt, 1987). A simpler procedure is a grid-search technique. For each couple  $(D_{10}, \lambda_0)$  in a fine two-dimensional grid (its borders are suggested by the data) we calculate the residual sum of squares RSS. Couple  $(D_{10}, \lambda_0)$  with the smallest RSS is considered to be 'the best'. The fitting procedure for  $D_1$  and  $\lambda$  is repeated for each value of  $K$  in the reasonable range. The corresponding values of RSS are compared.

### Intergranule Fusion

The *pars intermedia* of rat pituitary presents a homogeneous tissue formed by closely associated polygonal cells with ovoid nuclei. Secretory granules of various electron densities fill most of the

cytoplasm, and are stained positively with an anti  $\beta$ -endorphin antibody (not shown). Apparent intergranule fusions were observed (Fig. 3, see arrow) in the *pars intermedia* preparations taken from 7 animals. The larger granule was typically electron lucent, the other being electron dense. It was usually localized to one part of the larger granule, or sometimes as a spherical structure inside the larger granule (Fig. 3, see arrowhead). The frequency of such events was relatively low. Out of 3144 secretory granules measured in 24 cells only 80 intergranule fusions were detected.

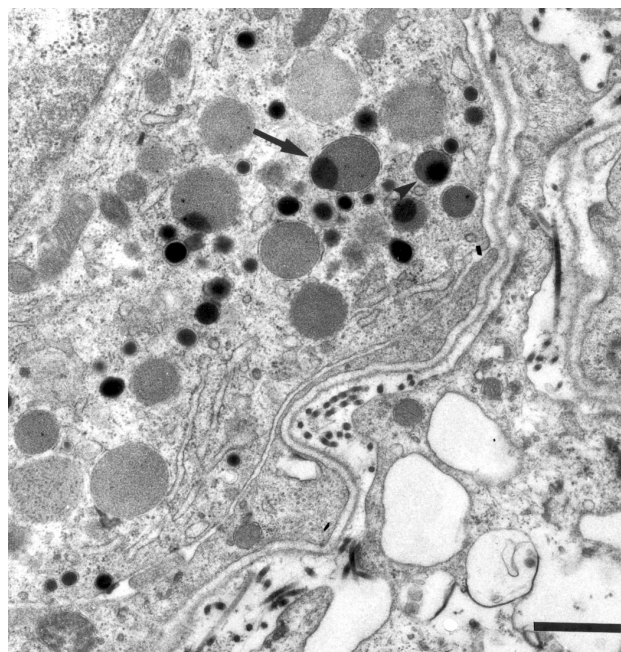


Fig. 3. Representative electron micrograph of a rat *pars intermedia* cell. Arrow indicates a tight association between two granules at an early step of (or just after) intergranule fusion. Arrowhead points to an electron dense inclusion in a secretory granule, possibly formed after a completion of intergranule fusion. Bar denotes 1000 nm.

### Distribution of Granule Diameters

Fig. 4A presents an empirical distribution of secretory granule profile diameters measured from 11 cells of the same animal. The distribution is skewed to the right consistent with the previous report (Zupančič *et al.*, 1994). Six other preparations show a similar distribution. The comparison of distributions from a single cell (Fig. 4B) and pooled cells of the same animal (Fig. 4A) indicates that the two distributions are similar. A potential multimodality may be anticipated in Fig. 4A.

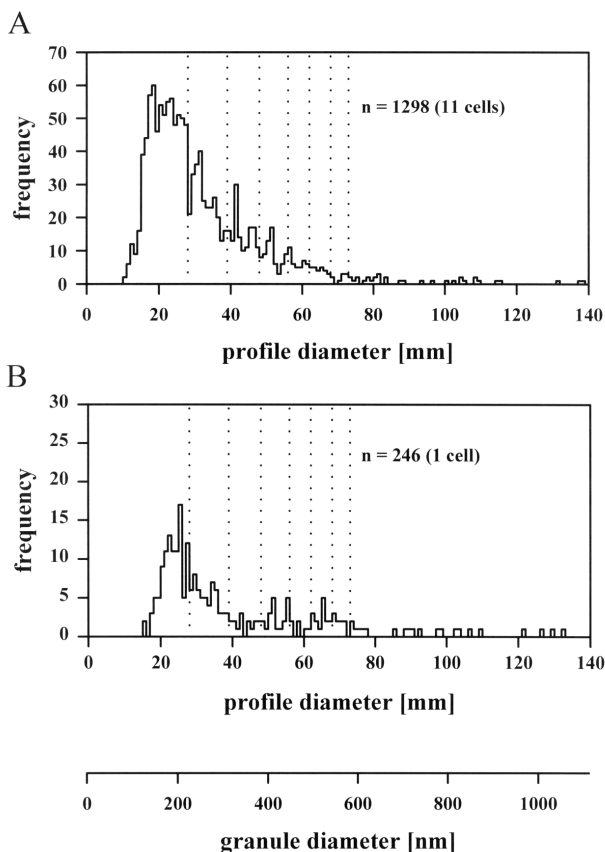


Fig. 4. Frequency distribution of secretory granule profiles obtained from 11 cells (Fig. 4A) and from 1 cell (Fig. 4B), all taken from the same animal. Dashed vertical lines represent values of estimated secretory granule diameters (see Table 2).

### Model Fitting

We tested whether the model presented in the Material and Methods could be a reasonable description of the empirical distribution presented on Fig. 5A. The measured profile diameters range from 11 to 139 mm (87 to 1103 nm). In the final statistical analysis seventeen granules (1.3%) with profile diameter larger than 84 (667 nm) were not included. The mean profile diameter for the remaining 1281 granules is 31.3 mm (248 nm), the standard deviation 13.9 mm (110 nm). The abscissa of the first possible peak is somewhere within 19-28 mm (151-222 nm).

### Fusion Effect Model

As described previously we used a simple grid-search procedure to find the estimates for  $D_1$  and  $\lambda$ . The grid was as follows: 10 mm to 30 mm with step 0.25 mm for  $D_1$ , and 0.10 to 4 with step 0.05 for  $\lambda$ . The search was repeated for each  $K = 2, 3, \dots, 9$ . The estimates accepted are:  $D_1 = 27.75$  mm,  $\lambda = 0.65$ . The RSS does not change considerably after  $K = 4$  (see Table 1).

Table 1. Residual sum of squares (RSS), estimate for granule diameter  $D_1$  (in mm) and  $\lambda$  for the maximal granular size type  $K = 2, 3, \dots, 7$ .

$K$	RSS	$D_1$ (mm)	$\lambda$
2	0.3919	30.00	0.65
3	0.2648	28.50	0.65
4	0.2226	27.75	0.65
5	0.2120	27.75	0.65
6	0.2101	27.75	0.65
7	0.2099	27.75	0.65

According to the results obtained the probability of appearance of unit granules is 0.522, the probability for double granules is 0.339, the probability of triple granules 0.110. The fraction of other granule types is negligible (see Table 2).

Table 2. Granule diameters  $D_k$  and its probability  $p_k$  for each granule size type  $k = 1, 2, \dots, 7$ . The results are based on the estimates:  $D_1 = 27.75$  mm,  $\lambda = 0.65$ ,  $K = 7$  (see Table 1).

$k$	1	2	3	4	5	6	7
$D_k$ (mm)	28	39	48	56	62	68	73
$p_k$	0.5220	0.3393	0.1103	0.0239	0.0039	0.0005	0.0001

The comparison of the relative cumulative function with its fit  $G$  (Fig. 5) shows that the model describes the empirical distribution considerably well up to approximately 37 mm, deviations increase afterwards. Fig. 4 presents dashed vertical lines, representing the expected position of granule diameters. Agreement of the expected positions and the actual peaks is not satisfactory.

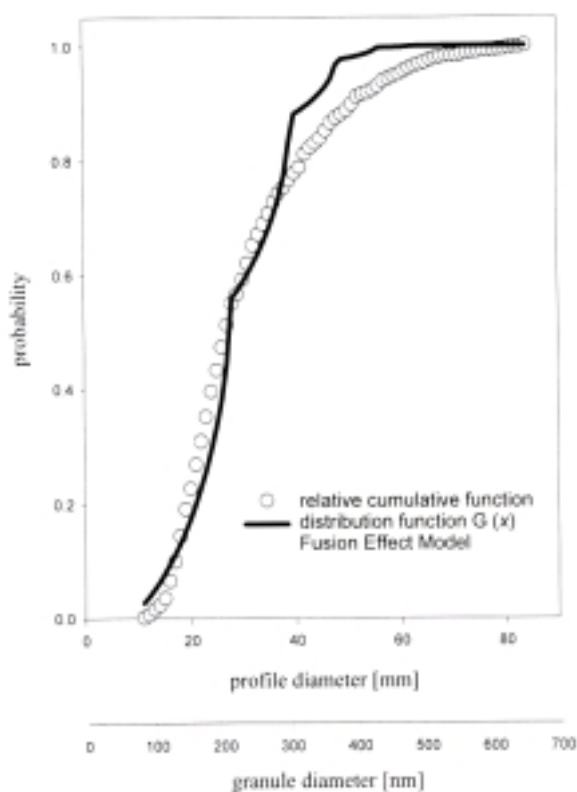


Fig. 5. Comparison of empirical data with the model in which intergranule fusion plays a role in granule size determination. Relative cumulative frequency (open circles) and its fit  $G$  (line) obtained on the basis of the following estimates:  $K = 7$ ,  $D_1 = 27.75$  nm,  $\lambda = 0.65$ . Residual sum of squares is 0.2099.

## DISCUSSION

Using electron microscopy, we studied the secretory granule morphology of rat *pars intermedia* cells. Morphological features representing intergranule fusion (Fig. 3) are among the clearest examples in comparison to those found in literature. The initiation of this process is indicated by a close association of two granules: a large, electron lucent, and a smaller, electron dense (Fig. 3, see arrow). On the other hand, an electron dense granule localized inside an electron lucent granule was also observed, indicating a completion of intergranule fusion (Fig. 3, see arrowhead).

The results are consistent with the previous studies. Farquhar *et al.* (1978) showed that packaging of prolactin into secretory granules involves aggregation of immature (smaller) granules forming larger ones. Fumagalli and Zanini (1985) describe that some mature secretory granules, located in somatomammotrophs, contain growth hormone and prolactin. Both are segregated in different portions of the granule, they

possibly originate from intergranule fusion. Moreover, the maturation of secretory granules in PC12 cells is associated by an increase in diameter from an average of about 80 nm to about 120 nm possibly due to intergranule fusion (Tooze *et al.*, 1991).

Morphological features of intergranule fusion in *pars intermedia* cells (Fig. 3) may also be involved in the maturation of secretory granules. Different electron densities of the fused granules could be attributed to the metabolic status of their cargo changing during the process of granule maturation. Electron dense granules probably represent immature granules. Tanaka *et al.* (1991) showed immunocytochemically that POMC was selectively found in electron dense granules, whereas  $\alpha$ -MSH in electron lucent granules. This result is consistent with the view that these granules are biosynthetic and storage organelles (Mains *et al.*, 1987).

In electrophysiological studies intergranule fusion was interpreted to contribute to the multimodal distribution of amplitudes of unitary exocytic membrane capacitance events, which report the size of fusing granules (Alvarez de Toledo and Fernandez, 1990; Hartmann *et al.*, 1995). To test whether this mechanism also affects the distribution of granule size in rat melanotrophs, we developed a simple probabilistic model predicting the formation of larger granules is due to the fusion of unitary granules. The model accounts for the sectioning of secretory granules (Weibel, 1979). This problem was solved analytically. The peaks in the distribution of measured profiles are expected to occur in the sequence  $D, D\sqrt{2}, D\sqrt{3}, \dots$  (see Theoretical Model, see Fig. 4B, dashed vertical lines), however the empirical distribution does not confirm that satisfactory.

It should be noted that in addition to tissue sectioning, examination by electron microscopy incorporates other features introducing a nonestimable bias in the data. For example: sections are not infinitely thin, granule profiles are not always sharp, non-spherical granules were also observed in our study. The assumption that unitary granules are of a fixed size is an oversimplification. Other processes, such as fusion of microvesicles with secretory granules (Tooze and Tooze, 1986; Komuro *et al.*, 1987), may additionally affect the distribution of secretory granule diameters.

To sum up, our electron micrographs reveal compelling evidence in support of intergranule fusion in rat *pars intermedia* cells. In an attempt to analyze the contribution of intergranule fusion to secretory granule growth, we consider the hypothesis that larger granules result from fusion between smaller granules

of unitary size (Alvarez de Toledo and Fernandez, 1990; Hartmann *et al.*, 1995). We developed a simple probabilistic model to explain this type of fusion and electron microscopy data acquisition, simultaneously. The data obtained do not give evident results, the fit is unsatisfactory. Therefore we conclude that further work has to be undertaken to get to a more conclusive answer about the fusion theory.

### ACKNOWLEDGEMENTS

This work was supported by the grant #J3-6207-381 from The Ministry of Science and Technology, The Republic of Slovenia. We thank S. Grilc for cell cultures and N. Kuzmin for improving our English.

### REFERENCES

- Alvarez de Toledo G, Fernandez JM (1990) Patch-Clamp Measurements Reveal Multimodal Distribution of Granule Sizes in Rat Mast Cells. *J Cell Biol* 110: 1033-9.
- Bäck N (1989) The Effect of Bromocriptine on the Intermediate Lobe of the Rat Pituitary: an Electron Microscopic, Morphometric Study. *Cell Tissue Res* 255:405-10.
- Bäck N, Sojnila S, Virtanen I (1993) Endocytotic Pathway in the Melanotroph of the Rat Pituitary. *Histochem J* 25:133-9.
- Bäck N, Sojnila S (1994) Regulation of Secretory Granule Formation in Chronically Hypersecretory Melanotrophs in the Rat Pituitary. *Cell Tissue Res* 275:339-44.
- Everitt BS (1987) Introduction to Optimization Methods and Their Application in Statistics. Chapman and Hall, 42-8.
- Farquhar MG, Reid J, Daniell LW (1978) Intracellular Transport and Packaging of Prolactin: A Quantitative Electron Microscope Autoradiographic Study of Mammothrophs Dissociated from Rat Pituitaries. *Endocrinology* 102:296-311.
- Fumagalli G, Zanini A (1985) In Cow Anterior Pituitary, Growth Hormone and Prolactin Can Be Packaged in Separate Granule of the Same Cell. *Cell Biol* 100:2019-24.
- Hartmann J, Sceppek S, Lindau M (1995) Regulation of Granule Size in Human and Horse Eosinophils by Number of Fusion Events among Unit Granules. *J Physiol (Lond)* 484.1:201-9.
- Komuro M, Kiuchi Y, Shioda T (1987) Membrane Modification During Secretory Granule Formation in Rat Somatotrophs. *Eur J Cell Biol* 43:98-103.
- Mains RE, Eipper BA (1979) Synthesis and Secretion of Corticotropins, Melanotropins and Endorphins by Rat Intermediate Pituitary Cells. *J Biol Chem* 254:7885-94.
- Mains RE, Cullen EI, May V, Eipper BA (1987) The Role of Secretory Granules in Peptide Biosynthesis. *Ann NY Acad Sci* 493:278-91.
- Rusakov DA (1993) Estimation of the Size of Closed Cell Elements from Analysis of Their Random Plane Sections. *Biometrika* 49:141-9.
- Rupnik M, Zorec R (1992) Cytosolic Chloride Ions Stimulate  $Ca^{2+}$ -induced Exocytosis. *FEBS Lett* 303:221-3.
- Tanaka S, Nomizu M, Kurosuni K (1991) Intracellular Sites of Proteolytic Processing of Pro-opiomelanocortin in Melanotrophs and Corticotrophs in Rat Pituitary. *J Histochem Cytochem* 39:809-21.
- Tooze SA (1991) Biogenesis of Secretory Granules. Implications Arising from the Immature Secretory Granule in the Regulated Pathway of Secretion. *FEBS Lett* 285:220-4.
- Tooze SA, Flatmark T, Tooze J, Huttner WB (1991) Characterization of the Immature Secretory Granule, an Intermediate in Granule Biogenesis. *J Cell Biol* 115:1491-1503.
- Tooze J, Tooze SA (1986) Clathrin-coated Vesicular Transport of Secretory Proteins During the Formation of ACTH-containing secretory granules in AtT20 cells. *J Cell Biol* 103:839-50.
- Weibel ER (1979) Stereological Methods for Micrological Morphometry. New York: Academic Press, 67-185.
- Zupančič G, Kocmur L, Veranič P, Grilc S, Kordaš M, Zorec R (1994) The Separation of Exocytosis from Endocytosis in Rat Melanotroph Membrane Capacitance Records. *J Physiol (Lond)* 480.3:539-52.